JTTEE5 6:211-216

Influence of Dopant on the Behavior under Thermal Cycling of Two Plasma-Sprayed Zirconia Coatings Part 2: Residual Stresses

R. Hamacha, P. Fauchais, and F. Nardou

The evolution of coating morphology and surface residual stresses was followed for three different powders: zirconia stabilized with 8 wt% yttria (YSZ), 9.9 wt% dysprosia (DSZ), and 9.8 wt% ytterbia (YbSZ). The YSZ reference powder was fused and crushed (-45 +22 μm), and the other two were agglomerated and sintered (-90 +10 μm). According to the size distributions and manufacturing process, the plasma-sprayed YSZ particles were fully molten, resulting in dense coatings with good contact between the splats; the DSZ and, especially, the YbSZ particles were partially molten.

In general, the surface residual stresses were slightly compressive before thermal cycling. The YSZ and DSZ coatings were insensitive to aging (600 h in air at room temperature), as shown by the surface stress evolution, which was not the case for YbSZ coatings. Six hundred furnace thermal cycles from 1100 °C to room temperature indicated excellent behavior of YSZ and DSZ coatings, with almost no variation of surface residual stresses, compared to a high dispersion for YbSZ coatings with the development of macrocracks parallel and perpendicular to the substrate within the coating.

Keywords residual stresses, thermal cycling, zirconia coating

1. Introduction

RESIDUAL stresses are among the most important parameters that determine the lifetime of thermal barrier coatings (TBCs) (Ref 1-11). These stresses can arise from the quenching of individual splats, the expansion mismatch between coating and workpiece, and the thermal gradients within the coating and substrate during spraying. Such stresses can result in coating spallation due to crack propagation parallel to the workpiece surface. Many studies have examined the behavior of yttria- or ceria-stabilized or partially stabilized zirconia coatings under various thermal cycling conditions, but no work has been reported on dysprosia and ytterbia partially stabilized zirconia. The current work is related to the behavior of such coatings when cycled in a furnace with air atmosphere at 10^5 Pa between 1100 °C and room temperature.

2. Experimental Procedure

The characteristics of the zirconia powders (-90 +10 μm) partially stabilized with dysprosia (DSZ) or ytterbia (YbSZ) and the spraying parameters have been detailed elsewhere (Ref 12). For comparison purposes, zirconia coatings stabilized with 8 wt% yttria (YSZ) were sprayed using fused and crushed particles with a smaller size distribution (-45 +22 μm) (Ref 12). With this powder, the contact between the splats is much better due to good particle melting, and the thermophysical properties of the coatings are improved compared to those obtained with YbSZ and DSZ coatings.

For the present study, the coatings were sprayed on disk-shaped (25 mm diam, 5 mm thick) $FeCr_{22}Al_{5.8}$ (PM alloy obtained by powder metallurgy) substrates grit blasted prior to spraying with Al_2O_3 grit (1.4 mm diam) at a pressure of 0.3 MPa, resulting in $R_a \approx 14$ to 15 μm. The coatings were sprayed with substrate preheating of 300 °C (Ref 12), and on completion of the spray operation, the plasma jet and the cooling air jets were switched off and the coating and substrate cooled slowly (over approximately 5 min) to room temperature.

The thickness of the coatings was close to 400 μm, and the as-sprayed coating roughness, estimated with a perthometer Mitutoyo surftest 201 (Mitutoyo, Japan), was about 10 μm. Coating surface strain measurements were performed using an X-ray device (PSI device: Dosophatex type, Courbon Co., St. Etienne, France), with an iron target in the case of the DSZ and YSZ coatings or a chromium target in the case of the YbSZ coating. The linear detector was equipped with a vanadium filter (12.5 μm thick).

3. Stress Determination

The residual stresses were measured by monitoring the shift of selected diffraction peaks (Ref 1, 3, 4, 13, 14). The lattice strain was obtained from the shift of a (hkl) peak, when compared with that for a corresponding unstrained specimen, a method employed by Castex and Sprauel (Ref 15). Measurement of the peak shift along the three angles, θ, Φ, and Ψ (Fig. 1), allows determination of the nine components of the stress

R. Hamacha, P. Fauchais, and **F. Nardou**, LMCTS—URA CNRS 320, 123 Avenue Albert Thomas, 87060 Limoges Cedex, France, Fax 55.45.75.86.

Part 1 of this article was printed in the *Journal of Thermal Spray Technology*, Vol 5 (No. 4), 1996, p 431-438.

tensor (Fig. 2). However, it must be emphasized that this method has a few drawbacks: (1) The limited penetration depth of x-rays (typically in the 5 μm range for zirconia) implies that stresses are measured within a region that is subject to stress relaxation, and (2) the layer removal technique to obtain the stress distribution within the coating is subject to errors since the stress distribution changes (Ref 14). Therefore, in this work no layer removal method was employed. The deformations were measured by using the X-ray diffraction (XRD) peaks of a single phase. It was thus important to know which crystalline phases were present together with the corresponding diffracting planes. The spectra obtained with the Kα copper radiation showed that the coatings consisted mainly of the nontransformable tetragonal phase, generated by very rapid cooling (>10 K/μs) during the spraying process (Ref 16).

In the case of the DSZ coating (measurements performed with an iron target), the (422) plane was chosen for determination of stresses, according to the corresponding line intensity and its angular position. However, since the intensity of the (224) peak was about one-third of the height of the peak (422) (Fig. 3a), deconvolution of the two peaks was mandatory. These angular ranges were used:

- θ: 64.5 to 71° by steps of 0.02° to obtain one spectra for given values of Ψ and Φ
- Ψ: −54 to 54° by steps of 9° (i.e., 13 θ scanning for a given Φ)
- Φ: 0 to 90° by steps of 45° (i.e., 3 scanning in θ for a given Ψ)

After smoothing the 39 patterns obtained (3 × 13), the deconvolution was performed assuming the two diffraction peaks had Gaussian shapes. The determined values were used to evaluate the deformation of the reticular planes:

$$\varepsilon_n^* = \frac{d_n^* - d_0}{d_0}$$

where d_n is the reticular plane distance in the n direction, and d_0 is the reticular plane distance in the z direction perpendicular to the sample surface (see Fig. 1).

To calculate the stresses, assuming elastic behavior, determination of the elastic constants E (Young's modulus) and ν (Poisson's ratio) is a prerequisite. This can be performed by using, for example, a four-point beam flexion test for samples detached from their substrate (Ref 10) or an ultrasonic method. Such measurements were performed (Ref 11) on YSZ coatings sprayed under similar conditions as those used in this study. There was no substrate preheating and the coating and substrate temperatures were kept below 200 °C during spraying, resulting in poor contact between splats (Ref 17). The Young's modulus of the plasma-sprayed YSZ coatings was 48 GPa, approximately 25% of the value of sintered zirconia (200 GPa). McPherson (Ref 18) interpreted this low value as due to the relatively low fraction of the "true" contact between the layered splats.

According to the particular microstructure of plasma-sprayed coatings, crystallographic data on elastic constants deduced from XRD experiments and those calculated with Kroner's model (Ref 19), for example, are very different from those determined by using the experimental values of E and ν (from four-point bending, ultrasonic tests, etc.). Thus, as emphasized by Zaouali (Ref 10), for precise stress determination it is necessary to know the crystallographic constants of the material. This was not possible in the present work, and the values proposed by Zaouali were used. The values were determined by studying the shift of (hkl) peaks when a tensile stress was applied to the plasma-sprayed coatings. Calculation of the corresponding values of E and ν showed that $E = 210$ GPa and ν = 0.31. Compared to E and ν values measured by the four-point method, E is about four times greater. This can be explained by the fact that, at the grain size scale, the grain behaves like a monocrystal, while the macroscopic measurements take into account all the macroscopic defects. The following crystallographic constants were used:

$$S_1 = -1.476 \times 10^{-6}$$

$$S_2 = 1.2476 \times 10^{-5}$$

When $\sigma_{33} = 0$, S_1 and S_2 allowed determination of the relationship between ε_n and the stress components σ_{11} and σ_{22}. The stress tensor was then obtained by performing a multiple regression and using Hooke's law ($\varepsilon_n = F_{ij} \times \sigma_{ij}$), where F_{ij} depended only on the crystallographic constants. It was assumed that these values remained constant whatever the type of coating and the number of thermal cycles, and this may not necessarily be true. The normal stress to the surface was assumed to be zero (the

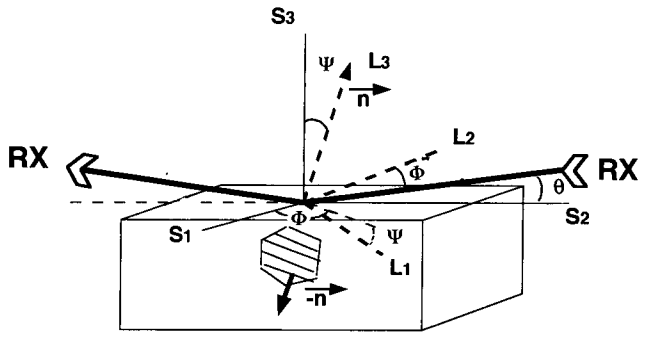

Fig. 1 Schematic depiction of the XRD technique for measurement of residual stresses, with definitions of the angles θ, Φ, and Ψ

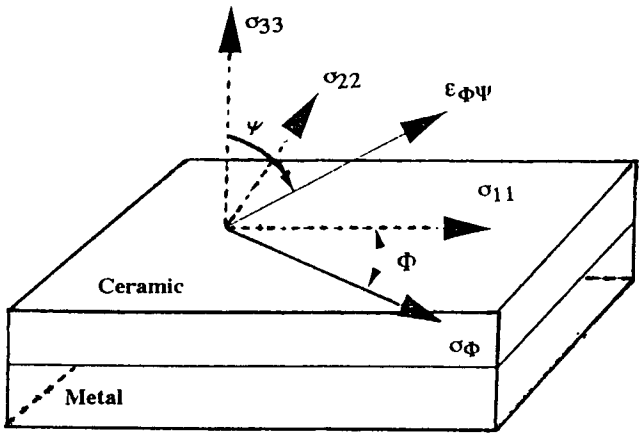

Fig. 2 Relative positions of the global stress and its main components referred to the measured strain $\varepsilon_{\Phi\Psi}$. The σ_{ij} components correspond to the shear stresses.

penetration of X-rays is less than 6 μm for zirconia; see Table 1), and d_0 was calculated for $\Psi = 0$.

A chromium target was used to study the YbSZ coatings, and the $(400)_{t'}$ plane was examined (Fig. 3b). No deconvolution was needed since the peak was isolated. The spectra obtained were processed automatically with house-developed software (Ref 20). In this case, the θ angular range was from 60 to 67° and was scanned by steps of 0.02°. The values of Φ and Ψ were the same as those used for DSZ.

4. Results

4.1 *Coating Surface Residual Stresses before Thermal Cycling*

The stress tensors obtained for each coating are given in Table 2. As anticipated, the stress values are weak because stresses generated during plasma spraying are relaxed, as shown by the microcracked state of the coatings. During the cooling of each

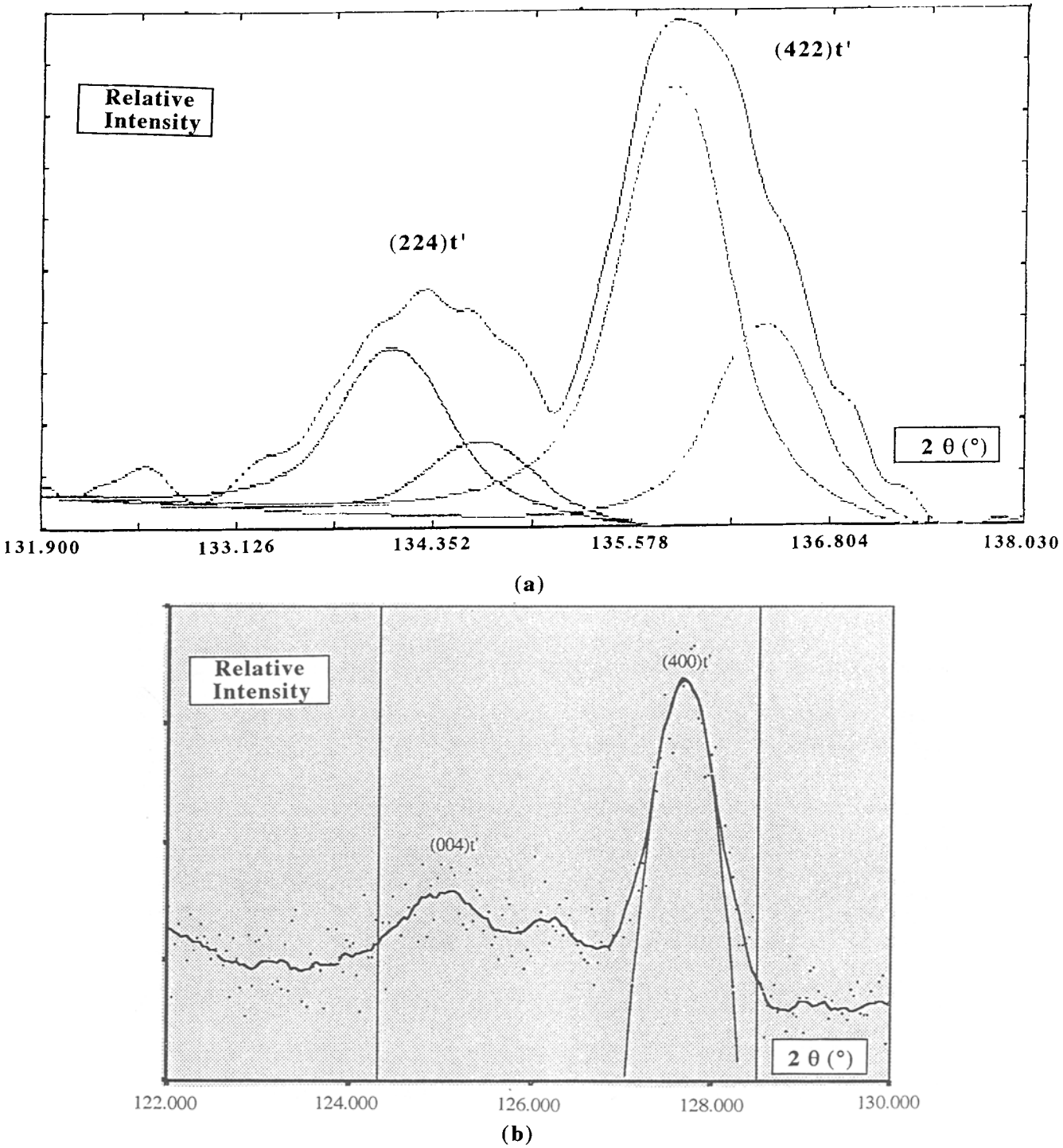

Fig. 3 Examples of XRD spectra for residual stress determination. (a) DSZ. (b) YbSZ

splat after solidification, tensile quenching stresses, σ_q, are generated. This stress can be approximated by:

$$\sigma_q = E_d \times \alpha_d \times \Delta T$$

where E_d is the Young's modulus of the coating, α_d is its volumetric expansion coefficient, and ΔT is the temperature difference between the plastic state of the particle (corresponding roughly to $T_p = 0.6 \times T_m$, where T_m is the melting temperature of the sprayed material) and that of the substrate ($T_s \sim 600$ K). The corresponding values for $\Delta T = T_p - T_s$ can be relaxed only by microcracks—as shown, for example, by the microcrack network observed by Bianchi et al. (Ref 21) for splats collected on hot (400 °C) substrates. According to Kuroda et al. (Ref 22), the residual quenching stress should be on the order of 10 to 20 MPa.

Two other types of stress exist in the substrate close to its surface: (1) the compressive stresses due to grit blasting and only partially (≈10%) relaxed by rapid preheating (90 to 120 s) of the substrate prior to spraying and the substrate heating during spraying (~300 s), and (2) residual stresses in compression gen-

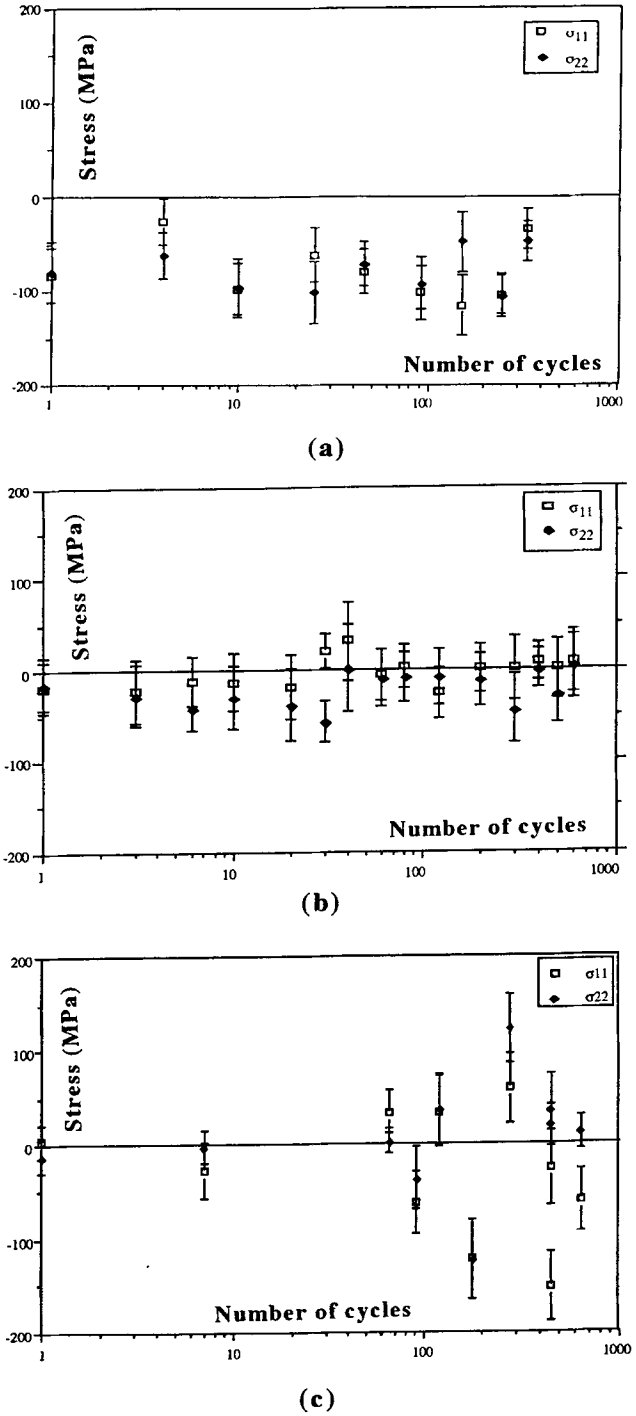

Fig. 4 Residual stress evolution with thermal cycling. (a) YSZ. (b) DSZ. (c) YbSZ

Table 1 Linear absorption coefficient and average penetration depth of X-rays in zirconia (at $\Psi = 0$ and $I/I_0 \approx 63\%$)

Parameter	Iron target	Chromium target
Linear absorption coefficient(a), m^{-1}	87,753	170,950
Average penetration depth of X-rays(b), μm	5.3	2.6
θ ZrO_2, deg	63.86	86.01
$(hkl)_t$	(422)	(400)

(a) Calculated with $\rho = 5700$ kg/m^3 for zirconia. (b) Calculated with the formula given in Ref 19.

Table 2 Influence of zirconia dopant on plasma coating surface residual stresses

Coating	Residual stress, MPa: Stresses tensor ± standard deviation	Main stresses
YSZ	$\begin{pmatrix}38 & 57 & 15\\ 57 & 3 & -21\\ 15 & -21 & 0\end{pmatrix} \pm \begin{pmatrix}31 & 20 & 6\\ 20 & 38 & 6\\ 6 & 6 & 19\end{pmatrix}$	$\sigma_{11} = -52$ $\sigma_{22} = 80$ $\sigma_{33} = 13$
DSZ	$\begin{pmatrix}67 & 12 & 64\\ 12 & -26 & -43\\ 64 & -43 & 0\end{pmatrix} \pm \begin{pmatrix}38 & 22 & 7\\ 22 & 42 & 8\\ 7 & 8 & 22\end{pmatrix}$	$\sigma_{11} = 10$ $\sigma_{22} = 107$ $\sigma_{33} = -76$
YbSZ	$\begin{pmatrix}27 & -33 & 1\\ -33 & 5 & 22\\ 1 & 22 & 0\end{pmatrix} \pm \begin{pmatrix}25 & 14 & 4\\ 14 & 25 & 4\\ 4 & 4 & 14\end{pmatrix}$	$\sigma_{11} = 54$ $\sigma_{22} = -31$ $\sigma_{33} = 9$

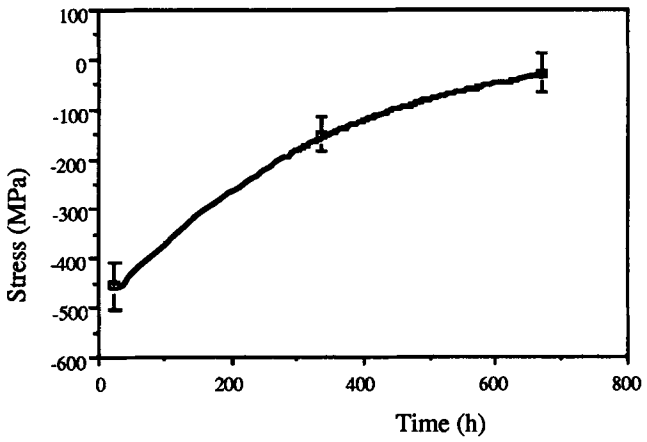

Fig. 5 Effect of aging on the superficial residual stresses of the YbSZ coating measured by XRD

erated within the coating upon cooling after spraying, assuming that the coating and substrate temperature remains uniform. However, the cooling temperature is not at all uniform, especially with the low thermal conductivity zirconia (≈3 W/m · K), and the coating surface cools faster than its bulk, resulting in extra tensile stresses at the surface. The tensile stresses, as summarized in Table 2, were confirmed by using the incremental hole drilling method (Ref 23) for alumina coatings sprayed on steel.

It is readily apparent that the stress tensor, no matter the stabilizer, exhibits shear stress components, σ_{ij}, which are not negligible compared to the main components, σ_{ii}. Moreover, the strain measured is on the order of 4×10^{-4} and corresponds to a peak shift of 6% in degrees (the measuring step in 2θ is 0.04°). The YSZ and DSZ coatings exhibit fewer cracks than the YbSZ coating, and the stress values are slightly higher. However, the same crystallographic constants S_i were used for the three stabilizers, and work is in progress to determine the validity of this assumption.

4.2 *Residual Stress Evolution with Thermal Cycling*

Globally, the surface stresses are slightly compressive in cycled coatings, as shown in Fig. 4, because of the thermal origin of these stresses. The YSZ coating exhibits the highest compressive stress due to the excellent contact between the splats (Fig. 4a), and, according to the precision of the measurements, it remains constant during thermal cycling. The coating undergoes no microscopic or macroscopic degradation during cycling, except for the creation of a few macrocracks orthogonal to the substrate. It appears that the DSZ coating exhibits relatively low stresses with very little variation during thermal cycling (Fig. 4b). It is worth noting that this coating, which is minimally constrained during all the cyclings, undergoes no macroscopic or microscopic degradation (Ref 9). Compared to YSZ coatings, the contact between the splats is somewhat inferior because some of the particles are not completely molten upon impact. Polished cross sections of the DSZ coatings reveal several large pores, corresponding to unmolten particles that have been pulled out; this is not the case with the YSZ coating. Just as for YSZ coatings, after thermal cycling of DSZ coatings a few macrocracks orthogonal to the substrate, starting from a large pore, are visible in polished cross sections.

For the YbSZ coating (Fig. 4c), taking into account the fact that the penetration of the X-rays is only 3 μm (chromium target) while the coating roughness is 10 μm, a dispersion of some measurement points is observed, particularly for the cycle numbered 449. At this cycle, two very different values (about –150 and –40 MPa) are obtained due to superficial aging of the coating at ambient temperature, which is enhanced by the thermal cycling. The coating cross section after thermal cycling (Ref 12) reveals decohesion with much larger cracks (compared to the two other coatings) perpendicular and parallel to the substrate.

According to the poor contact between the splats, this coating is sensitive to aging at room temperature due to humidity absorption. No aging effect on the superficial residual stresses was observed for the YSZ and DSZ coatings after 600 h in air, but this was not the case with YbSZ coating. Figure 5 shows that aging for this coating significantly decreases the superficial compressive residual stresses. The XRD measurements are very sensitive to this aging, especially when the penetration depth of the X-rays is low. The coating microstructure (microcracking, poor interlamellar contact, etc.) (Ref 12) can favor such stress relaxation. Furthermore, the microstructure in transverse sections of the coating cycled to 478 cycles appeared to be very heterogeneous and could also account for the observed dispersion. Thus, this coating undergoes high decohesion on thermal cycling, as indicated by its microstructure and microhardness values (Ref 9).

Measurements of the evolution of the *c/a* ratio with thermal cycling showed that after 600 cycles this ratio increased by 17.3% for DSZ and by 16.5% for YbSZ (Ref 12). Such an evolution, according to Miller and Lowell (Ref 24), is often linked to the decomposition of the t′ phase to c and m phases. In any case, XRD analysis revealed no increase of the m phase.

5. Conclusions

The DSZ coatings presented a very weak compressive surface stress (measured by XRD with an iron target), which remained stable during 600 furnace cycles from 1100 °C to room temperature. The evolution of the cell parameters during thermal cycling followed the same tendency as the surface stress, remaining almost constant.

The YbSZ coatings, with lower mechanical resistance ($HV_{5N} = 632 \pm 36$ compared to 695 ± 32 for the DSZ coatings), exhibited more dispersed values of surface residual stress after thermal cycling in connection with greater variations in its cell parameters. The coating microstructure, as revealed by cross-sectional examination, was quite heterogeneous with many macrocracks and microcracks, which can explain the observed dispersion and which are linked to the coating decohesion with thermal cycling.

References

1. M.K. Hobbs and H. Reiter, Residual Stresses in ZrO_2 + 8 wt% Y_2O_3 Plasma Sprayed Thermal Barrier Coatings, *Surf. Coat. Technol.*, Vol 34, 1988, p 33-42
2. R.A. Miller, Current Status of Thermal Barrier Coatings: An Overview, *Surf. Coat. Technol.*, Vol 30, 1987, p 1-11
3. U. Selvadurai and W. Reimers, Characterization of Phase Composition and Residual Stress State in Plasma Sprayed Ceramic Coatings, *High Performance Ceramic Films and Coatings*, P. Vincenzini, Ed., Elsevier, Amsterdam, 1990, p 319-328
4. R. Kingswell, K.T. Scott, and B. Sorensen, Measurement of Residual Stress in Plasma Sprayed Ceramic Coatings, *2nd Plasma Technik Symp.*, Vol 3, S. Blum-Sandmeier, H. Eschnauer, P. Huber, and A.R. Nicoll, Ed., Plasma Technik, Wohlen, Switzerland, 1991, p 377-388
5. R. Elsing, O. Knotek, and U. Balting, The Influence of Physical Properties and Spraying Parameters on the Creation of Residual Thermal Stresses during the Spraying Process, *Surf. Coat. Technol.*, Vol 41, 1990, p 147-156
6. J. Thornton, N. Ryan, and G. Stocks, The Production of Stresses in Thermal Barrier Coating Systems by High Temperature Oxidation, *Thermal Spray Industrial Applications*, C.C. Berndt and S. Sampath, Ed., ASM International, 1994, p 633-638
7. V. Teixeira, M. Andritschky, H. Grahn, W. Mallener, H. Buchkremer, and D. Stöver, Failure of PVD/Plasma Sprayed Thermal Barrier Coatings during Thermal Cycling, *Thermal Spray Science and Technology*, C.C. Berndt and S. Sampath, Ed., ASM International, 1995, p 515-520

8. R.A. Miller, W.J. Brindley, J.G. Goedjen, R. Tiwari, and D. Mess, The Effect of Silica on the Cyclic Life of a Zirconia Yttria TBC, *Thermal Spray Industrial Applications*, C.C. Berndt and S. Sampath, Ed., ASM International, 1994, p 49-55
9. R. Hamacha, B. Dionnet, A. Grimaud, and F. Nardou, Residual Stress Evolution during the Thermal Cycling of Plasma Sprayed Zirconia Coatings, *Surf. Coat. Technol.*, Vol 80, 1996, p 295-302
10. M. Zaouali, "XRD Characterization of Mechanical and Microstructural State of Metallic and Ceramic Thin Films Obtained by PVD and Plasma," Ph.D. thesis, ENSAM, Paris, 1990
11. M.C. Foujanet, "Study of ZrO_2-Al_2O_3 Coatings Plasma Sprayed," Ph.D. thesis, University of Limoges, Limoges, France, 1990
12. R. Hamacha, P. Fauchais, and F. Nardou, Influence of Dopant on the Behaviour under Thermal Cycling of Two Plasma Sprayed Zirconia Coatings, Part 1: Relationship between Powder Characteristics and Coating Properties, *J. Therm. Spray Technol.*, Vol 5 (No. 4), 1996, p 431-438
13. J.D. Lee, H.V. Ra, K.T. Hong, and S.K. Har, Analysis of Deposition Phenomena and Residual Stress in Plasma Spray Coatings, *Surf. Coat. Technol.*, Vol 56, 1992, p 27-37
14. J. Pina, A.M. Dias, V. Costa, A. Gonçalves, M. Zaouali, and S.L. Lebrun, Residual Stresses in Plasma Sprayed Coatings, *2nd Plasma-Technik Symp.*, Vol 2, S. Blum-Sandmeier, H. Eschnauer, P. Huber, and A.R. Nicoll, Ed., Plasma Technik, Wohlen, Switzerland, 1991, p 99-108
15. L. Castex and J.M. Sprauel, Recent Evolution of Residual Stresses Analysis by XRD, *Rev. Fr. Méc.*, Vol 2, 1987, p 103-110
16. S. Fantassi, M. Vardelle, A. Vardelle, and P. Fauchais, Influence of the Velocity of Plasma Sprayed Particles on Splat Formation, *J. Therm. Spray Technol.*, Vol 2 (No. 4), 1993, p 379-384
17. A. Vardelle, M. Vardelle, P. Fauchais, and P. Gobin, Monitoring Particle Impact on a Substrate during Plasma Spray Process, *NATO ASI Ser. E: Appl. Sci.*, Vol 282, 1995, p 95-129
18. R. McPherson, A Review of Microstructure and Properties of Plasma Sprayed Ceramic Coatings, *Surf. Coat. Technol.*, Vol 39/40, 1989, p 173-182
19. L. Castex, J.L. Lebrun, G. Maeder, and J.M. Sprauel, *Publications scientifiques et techniques*, ENSAM, Paris, No. 22, 1981
20. B. Dionnet, "Influence of Residual Stresses on Oxidation of Refractory Alloys in Air at High Temperature," Ph.D. thesis, University of Limoges, Limoges, France, 1993
21. L. Bianchi, F. Blein, P. Luchese, M. Vardelle, A. Vardelle, and P. Fauchais, Effect of Particle Velocity and Substrate Temperature on Alumina and Zirconia Splat Formation, *Thermal Spray Industrial Application*, C.C. Berndt and S. Sampath, Ed., ASM International, 1994, p 569
22. S. Kuroda, T. Fukushima, and S. Kitahara, Significance of Quenching Stress in the Cohesion and Adhesion of Thermally Sprayed Coatings, *J. Therm. Spray Technol.*, Vol 1 (No. 4), 1992, p 325-332
23. M. Mellali, "Influence of Substrate Temperature and Roughness on the Adhesion/Cohesion of Plasma Sprayed Alumina Coatings and on the Residual Stresses within Coatings," Ph.D. thesis, University of Limoges, Limoges, France, 1995
24. R.A. Miller and C.E. Lowell, Failure Mechanisms of Thermal Barrier Coatings Exposed to Elevated Temperatures, *Thin Solid Films*, Vol 95, 1982, p 265-273